Carbohydrate Polymers 93 (2013) 246–255

Contents lists available at SciVerse ScienceDirect

Carbohydrate Polymers

journal homepage: www.elsevier.com/locate/carbpol

Viscoelastic properties of fibrinogen adsorbed onto poly(ethylene terephthalate) surfaces by QCM-D

Aleš Doliška[a,*], Volker Ribitsch[b,1], Karin Stana Kleinschek[b,1], Simona Strnad[a,1]

[a] Laboratory for Characterization and Processing of Polymers, Faculty of Mechanical Engineering, University of Maribor, Smetanova 17, SI-2000 Maribor, Slovenia
[b] Institute of Chemistry, Karl-Franzens-University Graz, Heinrichstraße 28/III, AT-8010 Graz, Austria

ARTICLE INFO

Article history:
Received 2 December 2011
Received in revised form 17 February 2012
Accepted 21 February 2012
Available online 23 March 2012

Keywords:
QCM-D
Fibrinogen
Adsorption
Modelling
Haemocompatibility

ABSTRACT

In presented study a new approach using QCM-D for biocompatibility determination was introduced. The adsorption of fibrinogen on PET and modified PET surfaces was monitored in situ using QCM-D. Protein layer thicknesses were estimated on the basis of a Voight based viscoelastic model. The hydrophilicities and morphologies of the surfaces were investigated using a goniometer and AFM. The results showed that PET surfaces coated with sulphated polysaccharides are more hydrophilic and more fibrinogen-repulsive than non-modified PET surfaces. QCM-D equipped with QTools modelling software is well-applicable to the characterisation of surface properties and can be optimised for biocompatibility determination.

1. Introduction

The increasing life expectancy of the general population is adding to the number of people worldwide in need of cardiovascular care; global demand for cardiovascular devices will, therefore, continue to rise (Takemoto et al., 2004). Although there has been more than 50 years of synthetic cardiovascular implant development and therapy adjustments, the same problems persist: haemolysis, thrombosis, thromboembolic complications, anticoagulation-related haemorrhage, infection, and pannus formation (tissue overgrowth). Therefore the development of haemocompatible biomaterials is still a very important challenge in material science. However, owing to the very complex influences of several experimental conditions on the in vitro alteration of blood, there is still a lack of viable in vitro tests and methods to evaluate biomaterials' blood compatibility. A wide variety of different testing systems and techniques are used in the development of new materials (Imai & Nose, 1972; Seyfert, Biehl, & Schenk, 2002; Streller, Sperling, Hübner, Hanke, & Werner, 2003; Takemoto et al., 2004; Yu, Wang, Wang, & Liu, 2000).

The majority of these methods differ in their designs and the types of in vitro systems used. Major changes can take place in blood as a result of the complex processes that occur in in vitro systems. Therefore, in many studies the in vitro haemocompatibility determinations were performed using blood protein adsorption onto artificial surfaces (Wu, Simonovsky, Ratner, & Horbett, 2005). Protein, especially fibrinogen, adsorption studies are often used to test the biocompatibility of materials (Hemmersam, Foss, Chevallier, & Besenbacher, 2005; Weber, Wendel, & Kohn, 2005). Fibrinogen is a 340 kDa, rod shaped blood plasma protein roughly 45 nm long and approximately 5–7 nm in diameter. Surface bound fibrinogen has been shown to have a key role in the adhesion of platelets to artificial surfaces, and platelet adhesion to artificial surfaces is mediated exclusively by surface-bound fibrinogen and does not seem to involve the other plasma adhesion proteins (Weber et al., 2005). Among all blood proteins, fibrinogen has a prominent role in coagulation and platelet adhesion (Bajpai, 2008). Therefore it is of importance that the surfaces of blood contacting devices show reduced fibrinogen adsorption, since fibrinogen is part of the clotting cascade and has an influence on platelet activation and blood coagulation in the system (Zhang et al., 2008). It was found (Sit & Marchant, 1999; Wu et al., 2005) that fibrinogen adsorbs more intensively at hydrophobic surfaces.

In vitro methods of evaluating materials' haemocompatibility using protein adsorption are usually time consuming; therefore there is a need for further progress in developing accurate, reliable and simple techniques to test materials' haemocompatibility in vitro (Streller et al., 2003), which in future could be standardised.

Polyethylene terephthalate (PET) is one of the most frequently used biomaterials in cardiovascular surgery. Non-modified solid

* Corresponding author. Tel.: +386 22207902; fax: +386 22207990.
E-mail address: ales.doliska@uni-mb.si (A. Doliška).
[1] Member of the European Polysaccharide Network of Excellence (EPNOE).

0144-8617/$ – see front matter © 2012 Elsevier Ltd. All rights reserved.
doi:10.1016/j.carbpol.2012.02.075

PET possesses moderate biocompatibility, which is insufficient for cardiovascular replacements. Diversified PET surface coatings have been proposed for cardiovascular devices, however, so far no surface modification has produced satisfactory results (Ratner, 2007). The most promising results have been achieved using the highly sulphated glycosaminoglycan heparin; however, even in these cases some unwanted events occur. Polysaccharides are increasingly used in medical applications. Their biological properties can be modified by chemical derivatization sulphating, which can improve their anticoagulant properties. It is already well known (Nishino, Aizu, & Nagumo, 1991; Nishino & Nagumo, 1992) that the presence of acidic groups like sulphate and/or carboxyl groups is related to anticoagulant and antithrombotic effects.

Therefore one possible way to improve the haemocompatibility of PET surfaces is a coating with sulphated polysaccharides with anticoagulant properties (Fasl et al., 2010; Gericke et al., 2011; Indest et al., 2009). The attachment of the functional layers can be done either by the covalent bonding of (Keuren et al., 2003; Kristensen, Rensmo, Larsson, & Siegbahn, 2003) or by the physical sorption of polysaccharides (Fasl et al., 2010; Gericke et al., 2011; Indest et al., 2009; Indest, 2007; Liu, He, & Gao, 2005).

It is well known from earlier studies (Sanchez, Elgue, Riesenfeld, & Olsson, 1995; Sanchez, Elgue, Riesenfeld, & Olsson, 1998) that the triggering of the blood plasma activation system in contact with foreign surfaces can be eliminated by using artificial materials modified or immobilized by heparin. It is also known however that heparin, owing to its origin, could cause some adverse effects in patients.

In this study two types of model PET films were modified by direct adsorption of sulphated polysaccharides showing anticoagulant properties. Fibrinogen adsorption was monitored by quartz crystal microbalance with dissipation monitoring (QCM-D) and evaluated using two different models (the Sauerbrey eq. and the Voight viscoelastic model), which gave fruitful information about the adsorbed layers' properties.

1.1. Voight based viscoelastic model with QCM-D and QTools

Dissipation measurements enable qualitative analysis of the structural properties of adsorbed molecular layers. Different materials can easily be compared and one can see whether the Sauerbrey relation will accurately approximate the adsorbed mass or not. When there is an increase in the dissipation shift and deviations in the normalized frequency ($\Delta f_n/n$) shifts, the Sauerbrey equation is no longer valid (Vogt, Lin, Wu, & White, 2004). With QCM-D technology quantitative analysis of the thickness, shear elastic modulus and viscosity of the adsorbed films is possible. This is achieved by combining frequency change (Δf) and dissipation change (ΔD) measurements from multiple harmonics (overtones) and applying simulations using a Voight-based viscoelastic model. The change in frequency is proportional to adsorbed mass; however this relation, known as the Sauerbrey relation, is valid only for rigid films. Dissipation is energy loss in the molecular layer on the sensor. This is measured by turning off the excitation voltage to the sensor, which causes the oscillation to decay. This decay of energy loss is related to the viscosity and elasticity of the molecular layer on the sensor.

In the case of viscoelastic or soft films the Sauerbrey relation underestimates the mass, since the film is not fully coupled to the motion of the sensor surface (Höök et al., 2001; Irwin, Ho, Kane, & Healy, 2005).

For rigid, thin and evenly distributed films the Sauerbrey relation is a good estimation in cases when the change in the dissipation factor $\Delta D < 1 \times 10^{-6}$ for 10 Hz frequency change (Kou, Tao, & Xu, 2010). In these cases the Sauerbrey equation (Sauerbrey, 1959) (Eq. (1)) can be used for adsorbed mass calculations:

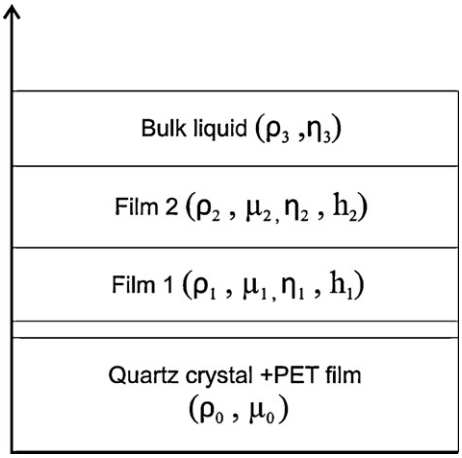

Fig. 1. Quartz crystal covered by two layers.

$$\Delta m = -\frac{C \cdot \Delta f}{n} \tag{1}$$

where C (17.8 ng cm^{-2} Hz^{-1}, when $n = 1$, $f_0 = 5$ MHz) is the constant (describing surface area, density and shear modulus of quartz resonator) and n is the overtone number.

From Sauerbrey masses (ng/cm^2) it is also possible to obtain the adsorbed layer thickness (Eq. (2)), however in this case the effective density of the adsorbed layer ρ_{ef} has to be estimated.

$$h_f(\text{nm}) = \frac{10^7(\text{nm/cm})\,\Delta m(\text{ng/cm}^2)}{10^9(\text{ng/g}) \cdot \rho_{ef}(\text{g/cm}^3)} \tag{2}$$

In the case of adsorbed soft films, the system energy dissipation increases. The dissipation factor D is proportional to the power dissipation of the oscillating system (Eq. (3)) and gives important information about the rigidity of the adsorbed layer (Kou et al., 2010):

$$D = \frac{E_{diss}}{2\pi E_{strd}} \tag{3}$$

where E_{diss} is the energy dissipated during one oscillation and E_{strd} is the energy stored in the oscillation system.

In cases when $\Delta D > 1 \times 10^{-6}$/10 Hz, an evaluation process based on the Voight model of viscoelasticity (Voight modelling) has to be used (Eqs. (4) and (5)) (Voinova, Rodahl, Jonson, & Kasemo, 1999).

$$\Delta f \approx -\frac{1}{2\pi\rho_0 h_0}\left\{\frac{\eta_3}{\delta_3}\sum_{j=1,2}\left[h_j\rho_j\omega - 2h_j\left(\frac{\eta_3}{\delta_3}\right)^2 \cdot \frac{\eta_j\omega^2}{\mu_j^2 + \eta_j^2\omega^2}\right]\right\} \tag{4}$$

$$\Delta D \approx \frac{1}{2\pi f\rho_0 h_0}\left\{\frac{\eta_3}{\delta_3}\sum_{j=1,2}2h_j\left(\frac{\eta_3}{\delta_3}\right)^2 \cdot \frac{\mu_j\omega}{\mu_j^2 + \eta_j^2\omega^2}\right\} \tag{5}$$

In the Voight viscoelastic model Δf and ΔD depend on the density (ρ), thickness (h), elastic shear modulus (μ) and shear viscosity (η) of the adsorbed layer (j: number of adsorbed layers) (Fig. 1).

The analysis software QTools contains both the Voight viscoelastic models, the Maxwell model and the Sauerbrey relation, thus allowing for characterization of soft and rigid films. It enables quantification of the film in terms of mass, thickness, water content, density and viscoelastic properties (Höök et al., 2001; Irwin et al., 2005).

Fitting was performed using a Simplex algorithm to find the minimum in the sum of the squares of the scaled errors between the

experimental and model Δf and ΔD values (Laos, Parker, Moffat, Wellner, & Ring, 2006).

The main aim of this study was to find out how different surface modifications of PET films influence fibrinogen adsorption and the adsorbed layer's thickness and morphology. The interdependence between adsorbed anticoagulant layers and the amount of adsorbed fibrinogen was evaluated using QCM-D and QTools software.

2. Materials and methods

2.1. Materials

Two types of polyethylene terephthalate (PET) surfaces were used. The first type was an untreated model PET film (PET), and the second one was a cationic PET surface (PET-P) with polyethylene imine (PEI) adsorbed onto the model PET film.

PET foil (Mylar®) with a thickness of 175 μm was used in the preparation of the model PET surfaces.

All chemicals used were of analytical grade and used without further purification.

Fibrinogen, Fraction I, Type III from human plasma (Sigma Aldrich, F4129) dissolved (1 mg/mL) in phosphate buffer saline (PBS; 6.44 mM KH_2PO_4, 8 mM Na_2HPO_4, 140 mM NaCl; pH 7.4) was used within the scope of the fibrinogen adsorption studies.

Heparin sodium salt from porcine intestinal mucosa (Fluka 51551) was used. Polyethylenimine (PEI), branched with average Mw ~25,000 (Aldrich 408727), was used in the preparation of PET-P surfaces.

Galactoglucomannan (GM) was recovered from the process water of spruce wood thermomechanical pulping (TMP) according to Willför, Rehn, Sundberg, Sundberg, and Holmbom (2003). The molecular mass of the recovered GM was around 40 kDa with a mannose/glucose/galactose unit ratio in the water-soluble spruce GM of approximately 4/1/0.5.

Thereafter GM was carboxymethylated (Doliška et al., 2011) and then both the GM and carboxymethylated GM were sulphated according to Doliška et al. (2011). The degree of sulphation (DS) for the sulphated GM was 0.81 and for the sulphated carboxymethyl GM the DS was 0.63.

2.2. Methods

2.2.1. Quartz crystal microbalance

All adsorption studies were performed using Quartz Crystal Microbalance with Dissipation monitoring apparatus, QCM-D (Model E4, QSense AB, Göteborg, Sweden). The method is based on monitoring the change in resonance frequency of a thin AT-cut piezoelectric quartz crystal disk that oscillates in the shear mode when AC voltage is applied across electrodes. The resonant frequency changes with the mass deposited on the crystal surface, rendering QCM a very sensitive mass sensor.

The quartz crystals (supplied by Q Sense AB) were AT-cut quartz with gold plated electrodes and with gold on the active surface. The fundamental frequency of quartz crystals is $f_0 \approx 5$ MHz and the sensitivity constant $C = 0.177$ mg/m^2 Hz.

2.2.2. Preparation of PET model surfaces

The spin coated PET films were prepared by dissolving 1 wt.% of PET foil in 1,1,2,2-tetrachloroethane (Fluka, 86960) and heating ($T \approx 150$ °C) until the foil dissolved. After the solution had cooled, it was filtered through a 0.2 μm Acrodisc GHP filter. 30 μL of solution was spread on a quartz crystal ($d = 14$ mm) and spin coated at a maximum of 2000 rpm for 60 s. After that the crystals were dried in a vacuum oven at 100 mbar and 30 °C overnight. The PET film thicknesses were estimated by measuring the change in frequency before and after spin coating in air with QCM-D and were found to be 48 ± 10 nm. Prior to spin coating, all crystals were cleaned in a 5:1:1 mixture of MQ water, H_2O_2 (30%) and NH_4OH (25%) for 5 min at 70 °C.

Prior to polysaccharide adsorption step, all crystals were rinsed again and constant frequency over longer period of time was observed, suggesting that PET film is stable and well attached to the quartz crystal.

PET-P surfaces were prepared from PET surfaces by adsorbing a 0.1% solution of the cationic polyelectrolyte PEI as an anchoring layer for sulphated polysaccharides.

2.2.3. Contact angle determination

The static water contact angles (WCA) of the model PET surfaces were determined with an OCA35 goniometer (Dataphysich, Germany). All measurements were done in at least 5 repetitions and the water drop volume was fixed to 3 μL.

2.2.4. Adsorbed layer topography evaluation

The topographical features of the modified surfaces were characterized by atomic force microscopy (AFM) in tapping mode with an Agilent 5500 AFM multimode scanning probe microscope (Digital Instruments, Santa Barbara, CA). The images were scanned using silicon cantilevers (ATEC-NC-20, Nanosensors, Germany) with a resonance frequency of 210–490 kHz and a force constant of 12–110 N/m. The scanned image size was 0.5 μm × 0.5 μm. All measurements were performed at ambient temperature in air.

2.2.5. Modifying PET surface through adsorption of PS

All adsorption studies were performed using QCM-D. The method is based on monitoring the change in resonance frequency of a thin AT-cut piezoelectric quartz crystal disk that oscillates in the shear mode when AC voltage is applied across electrodes. The resonant frequency changes with the mass deposited on the crystal surface, rendering QCM a very sensitive mass sensor.

The quartz crystals (supplied by Q Sense AB) were AT-cut quartz with gold plated electrodes and with gold on the active surface. The fundamental frequency of quartz crystals is $f_0 \approx 5$ MHz and the sensitivity constant $C = 0.177$ mg/m^2 Hz.

The modification of the PET model surfaces was performed in the QCM-D measuring chamber. Crystals coated with PET films were first washed with milliQ water at a flow rate of 0.2 mL/min for 20 min, after which the flow rate was lowered to 0.1 mL/min. When the frequency signal remained stable, the adsorption of polysaccharides followed as described in Table 1. Pure PET film in Table 1 is denoted for PET without an anchoring agent and PET-P is cationic PET film.

The concentrations of all polysaccharides were 100 mg/L and the concentration of $CaCl_2$ (when added) was 0.01 M. After adsorption of the polysaccharides, the QCM crystals were rinsed with milliQ water until constant frequency and dissipation signals were reached, so that the fibrinogen adsorption step would be performed on a system in equilibrium. Crystals with adsorbed polysaccharides were then dried in the flow of nitrogen and prepared for fibrinogen adsorption step, water contact angle measurements and AFM imaging. Such treatment enabled polysaccharide molecules to absorb irreversibly (Holmberg, Jönsson, Kronberg, & Lindmann, 2003).

The model PET films and PET-P films were treated as a rigid extension of the quartz crystal when estimations were done using the Sauerbrey equation.

2.2.6. Protein adsorption studies

For protein adsorption studies a solution of approximate in vivo concentration (Guicai, Xiaoli, Ping, Ansha, & Nan, 2008) 1 g/L human fibrinogen in PBS (pH 7.4) was used. Adsorptions were performed at 21 °C at constant flow (0.1 mL/min) in a Q-Sense standard flow

Table 1
Sample denotations and descriptions.

Sample denotation	Sample preparation
PET-H-Ca	PET model film coated with heparin in the presence of $CaCl_2$
PET-GM-Ca	PET model film coated with sulphated GGM in the presence of $CaCl_2$
PET-CMGM-Ca	PET model film coated by sulphated carboxymethyl GGM in the presence of $CaCl_2$
PET-P-H	PET model film modified by PEI and coated with heparin
PET-P-GM	PET model film modified by PEI and coated by sulphated GGM
PET-P-CMGM	PET model film modified by PEI and coated by sulphated CM GGM
PET-P-H-Ca	PET model film modified by PEI and coated by heparin in the presence of $CaCl_2$
PET-P-GM-Ca	PET model film modified by PEI and coated by sulphated GGM in the presence of $CaCl_2$
PET-P-CMGM-Ca	PET model film modified by PEI and coated by sulphated CM GGM in the presence of $CaCl_2$

module (QFM 401, QSense). Before protein adsorption all surfaces were rinsed with a PBS buffer for 20 min at a flow rate of 0.1 mL/min. All experiments were done in at least three repetitions.

3. Results and discussion

3.1. Haemocompatible PET surface preparation

Haemocompatible PET surfaces were prepared using two different approaches: by direct adsorption of anticoagulant agents (heparin and sulphated galactoglucomannans) onto the PET model film surfaces and by adsorption to a cationic PET surface (PET-P), with PEI as an anchoring layer onto which heparin and sulphated polysaccharides were adsorbed.

The adsorbed layer thicknesses were evaluated using the Sauerbrey equation, and the results are listed in Table 2.

When adsorption onto the PET surfaces was applied heparin (H), sulphated galactoglucomannan (GM) and sulphated carboxymethylated galactoglucomannan (CMGM) built layers with thicknesses between 2.0 and 3.5 nm (Table 2). It could be expected that high ionic strengths, owing to the presence of Ca^{2+} ions, influence the adsorption of anionic polysaccharide macromolecules in dense coiled conformation with incorporated Ca^{2+} and water molecules. From other studies (Dário, Hortêncio, Sierakowski, Neto, & Petri, 2011; Liu, Choi, Gatenholm, & Esker, 2011) is known that Ca^{2+} ions form strong bridges with negatively charged groups in PS and coiling thus more molecules can adsorb onto the surface, causing the change in frequency and dissipation.

Repulsive forces between the pure PET surface and coiled PS molecules cause higher desorption during the rinsing step. Therefore those surfaces remain more hydrophobic in comparison to the PET-P surface (Fig. 2).

The cationic PEI layer in the absence of Ca^{2+} ions caused the adsorbed polysaccharide layers to be much more densely packed.

The layer thicknesses of the adsorbed PS layers on PET-P were practically identical, as in the case of direct adsorption of polysaccharides onto PET in the presence of Ca^{2+}. Anionic polysaccharide macromolecules in solutions at low ionic strength adsorb in more or less extended conformation with a small adsorbed mass and occupy all the oppositely charged sites on the surface and form thin adsorbed monolayers with thicknesses of app. 3 nm.

Table 2
Thicknesses of polysaccharide layers (PS) (after rinsing with MQ-water), determined using the Sauerbrey equation.

Sample	Adsorbed PS layer thickness (nm)	Adsorbed mass (ng/cm^2)	Average surface roughness (nm)
PET-H-Ca	2.0 ± 1.0	200 ± 100	0.79
PET-GM-Ca	3.5 ± 1.0	350 ± 100	0.90
PET-CMGM-Ca	3.0 ± 1.0	300 ± 100	0.92
PET-P-H	2.5 ± 1.0	250 ± 100	0.98
PET-P-GM	2.5 ± 1.0	250 ± 100	1.18
PET-P-CMGM	4.0 ± 1.0	400 ± 100	1.10
PET-P-H-Ca	8.0 ± 4.0	800 ± 400	2.00
PET-P-GM-Ca	13. ± 5.0	1300 ± 500	2.10
PET-P-CMGM-Ca	14. ± 4.0	1400 ± 400	2.80

3.2. Contact angles of coated model PET films

Hydrophilicity changes in the PET surfaces before and after polysaccharide adsorption were analysed using water contact angle determination (Fig. 2). The results are represented in the diagram in Fig. 4. As expected, after polysaccharide adsorption the PET surfaces become more hydrophilic. The heparin layer only slightly decreased the contact angle of the PET surface. GM and CMGM adsorption however decrease the WCA by about 23% in comparison to the PET surface. The intermediate PEI layer caused a further decrease in the WCA. However, the highest hydrophilicities were achieved with polysaccharide layers when calcium chloride was present in the polysaccharide solutions during adsorption. As mentioned earlier, the high ionic strength of the polymer solutions influenced the more coiled conformations of the adsorbed molecules, and such structures in the adsorbed layers exhibit higher hydrophilicities, what was shown with water contact angle measurements and AFM imaging, where increased surface roughness was observed.

The increase in hydrophilicity of the modified PET surfaces has an important influence on fibrinogen adsorption. Cacciafesta, Humphris, Jandt, and Miles (2000) found that a hydrophobic surface promotes better adhesion of fibrinogen than either charged surfaces, whereas a hydrophilic negatively charged substrate produces the smallest perturbation to the protein native structure. Some other studies (Kannan, Salacinski, Vara, Odlyha, & Seifalian, 2006) have shown that the ideal water contact angle on a polymer surface for optimal endothelialisation with minimal platelet adhesion is 55°, and that the water contact angle directly demonstrated a polymer's thrombogenic potential (Kannan et al., 2006).

3.3. AFM images of surfaces

In Fig. 3 AFM images of the PET surface treated with PEI and haemocompatible polysaccharides with and without addition of calcium chloride are shown.

It can be seen from the AFM images and calculated average roughness's (Sa), that the Sa increased after the polysaccharides adsorption onto PET. The highest increase in average roughness was noted in the PET-P-GM and PET-P-CMGM samples and much higher in cases when calcium chloride was added. In these cases grained structure was observed, most likely due to polysaccharide adsorption in a coiled conformation owing to the presence of Ca^{2+} ions. Besides chemical surface modifications, physical changes in the surfaces (i.e. the differences in average surface roughness) significantly influenced the surface hydrophilicity.

3.4. Fibrinogen adsorption

Diagrams showing frequency and dissipation changes during fibrinogen adsorption are presented in Figs. 4–9.

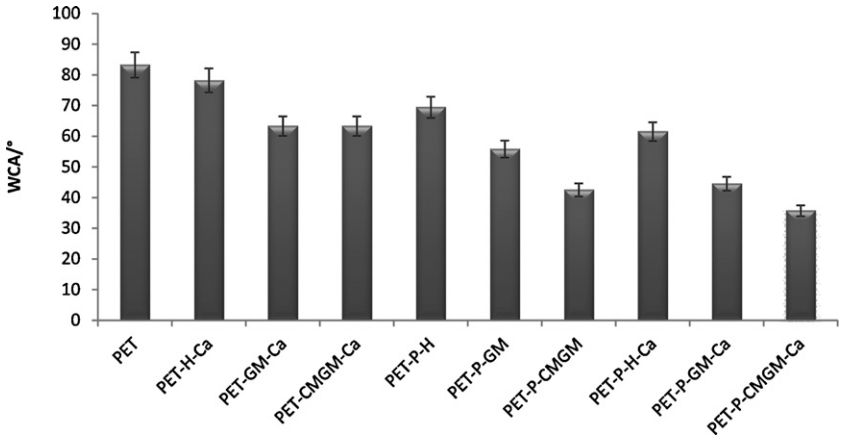

Fig. 2. Water contact angles (WCA) of non-modified (PET) and differently modified PET surfaces.

There were significant differences in fibrinogen adsorption onto PET surfaces modified with different sulphated polysaccharides (Fig. 4). It can be clearly seen from Fig. 4 that fibrinogen adsorption on the pure PET surface caused the maximum changes in frequency as well as in dissipation, indicating the maximum adsorption. GM-Ca in contrast caused the minimum fibrinogen adsorption. The fibrinogen adsorbed immediately after it was introduced to the system in all cases. By comparing the frequency change versus dissipation change during fibrinogen adsorption onto differently modified model PET films (Fig. 5), valuable information on the viscoelastic properties of the adsorbed layers can be obtained.

$\Delta D = f(\Delta f)$ plots provide an indication of how newly added mass affects the adsorbed layer's structure (Indest, Laine, Kleinschek, & Zemljic, 2010). In other words, information about what kind of layer (soft, rigid) was formed by the adsorption can be obtained. The lower the slope of the function (k), the more dense and rigid is the layer and, on the other hand, high k values indicate softer and more dissipating layers. The kinetics of fibrinogen adsorption onto the non-modified PET showed three somehow separate phases (slopes), which suggested direct adhesion and orientation changes associated with hydrodynamically coupled water (Kou et al., 2010). The first slope of the function (k_1) was 0.21×10^{-6}/Hz, the second

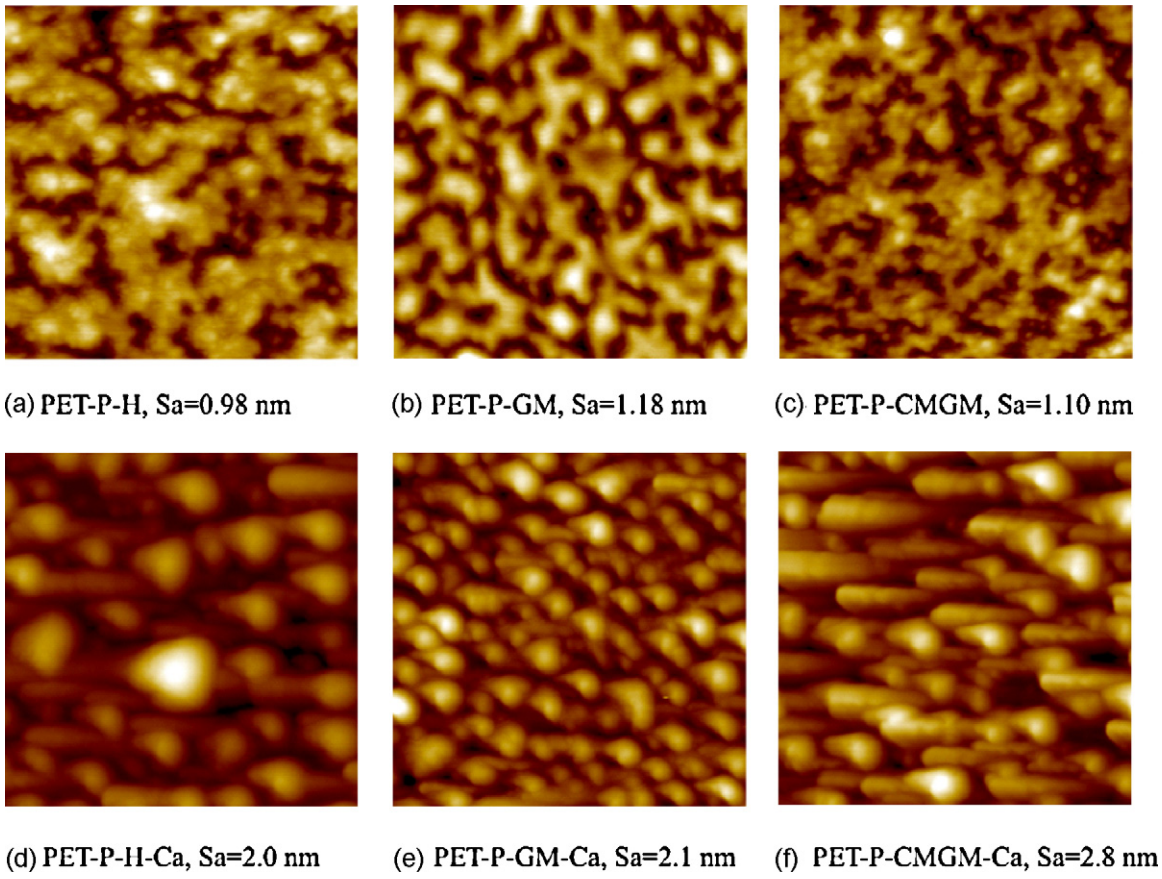

Fig. 3. AFM topography images of PET film surfaces and average surface roughness (Sa): (a) heparin adsorbed on PET-P film, (b) sulphated GM adsorbed on PET-P film, (c) sulphated CMGM adsorbed on PET-P film, (d) heparin adsorbed on PET-P film in presence of Ca^{2+}, (e) sulphated GM adsorbed on PET-P film in presence of Ca^{2+}, (f) sulphated CMGM adsorbed on PET-P film in presence of Ca^{2+}.

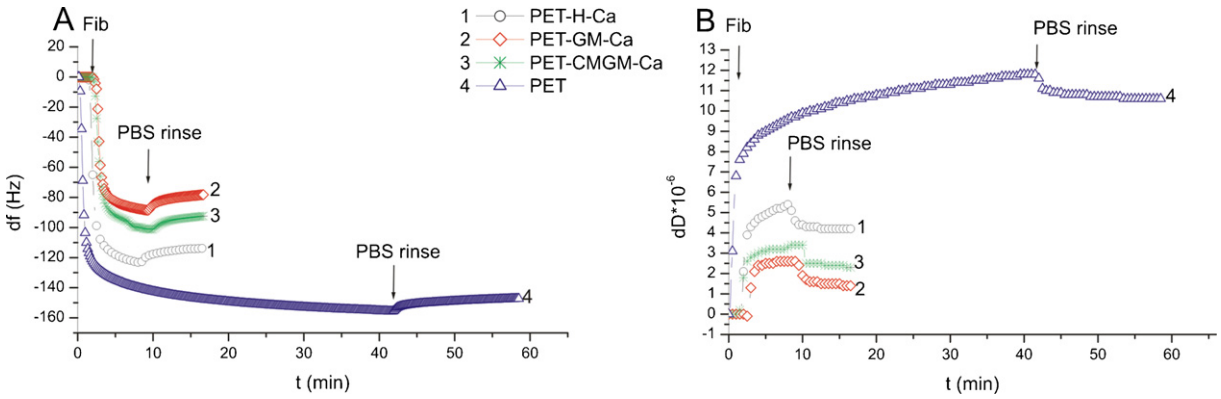

Fig. 4. Frequency (A) and dissipation (B) changes as a function of time during fibrinogen adsorption onto model PET surfaces coated with heparin (H), sulphated GM and sulphated CMGM in presence of Ca^{2+} ions.

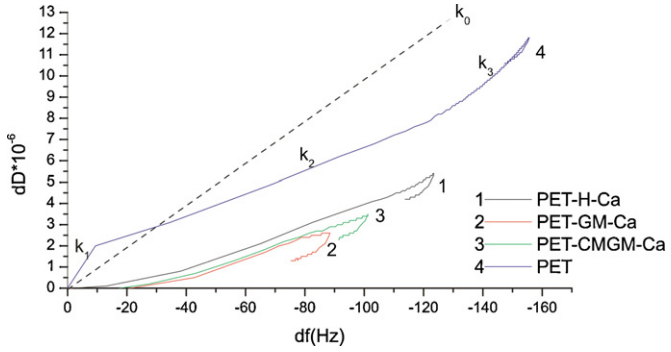

Fig. 5. $\Delta D = f(\Delta f)$ functions of fibrinogen adsorption onto model PET films modified with polysaccharides in the presence of Ca^{2+} (k_1, k_2 and k_3 – slopes different to that of function 4; k_0 – theoretical function slope, which indicates the boundary between soft and rigid adsorbed layers).

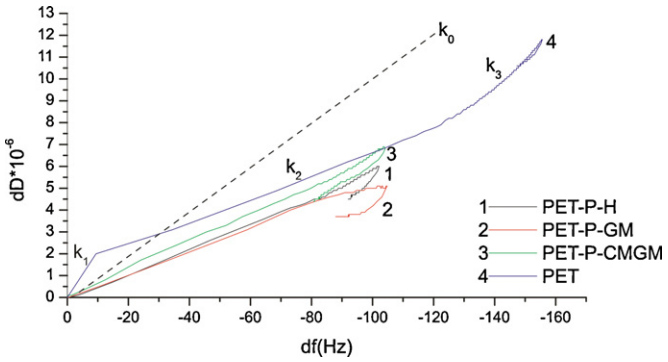

Fig. 7. $\Delta D = f(\Delta f)$ functions of fibrinogen adsorption onto model PET-P films modified with polysaccharides (k_1, k_2 and k_3 – different slopes compared with function 4; k_0 – theoretical function slope, which indicates the boundary between soft and rigid adsorbed layers).

slope (k_2) 0.06×10^{-6}/Hz and the third one (k_3) 0.13×10^{-6}/Hz. This indicated that at the beginning adsorption was very fast, but then quickly reduced to values similar to those of the modified PET surfaces. The third slope value is again higher, owing to the faster deposition of mass, indicating a change in conformation of the adsorbed fibrinogen or even possible multilayer adsorption. The slopes of the function $\Delta D = f(\Delta f)$ of fibrinogen adsorption onto the PET surfaces modified with sulphated polysaccharides in the presence of Ca^{2+} were all practically equal (0.05×10^{-6}/Hz), linear and far below the slope k_0, the "soft–rigid" boundary. Slopes higher than k_0 indicate soft, water rich adsorbed film, while slopes smaller than k_0 represent more rigid and densely adsorbed layers.

Fig. 6 represents the frequency and dissipation change during adsorption of fibrinogen onto the PET-P surfaces modified with sulphated polysaccharide adsorption. The results showed significant differences between the non-modified and modified samples, whereby the frequency changes were about 50% smaller for the modified samples. After rinsing, there were no significant differences in frequency changes between the three modified samples.

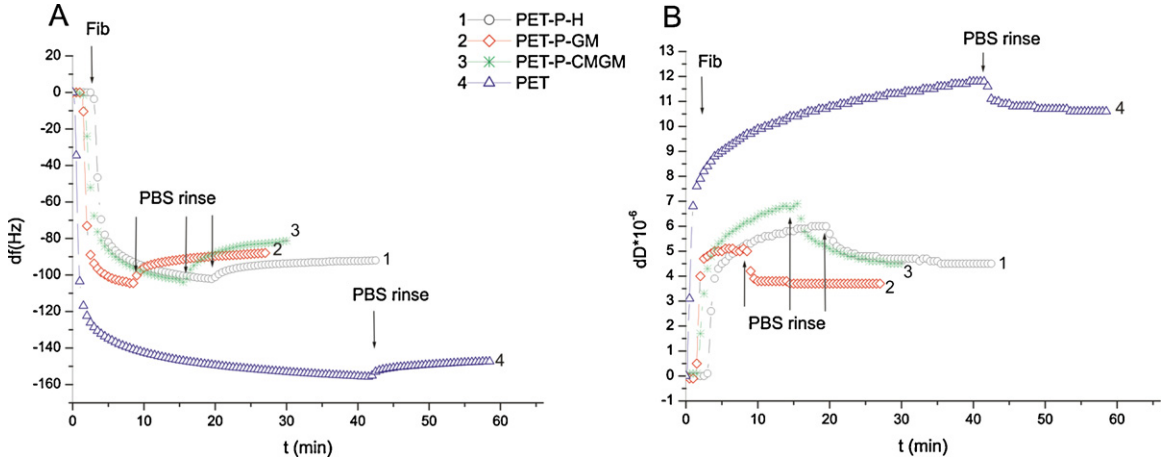

Fig. 6. Frequency (A) and dissipation (B) changes as a function of time during fibrinogen adsorption onto model PET-P surfaces coated with heparin (H), sulphated GM, and sulphated CMGM.

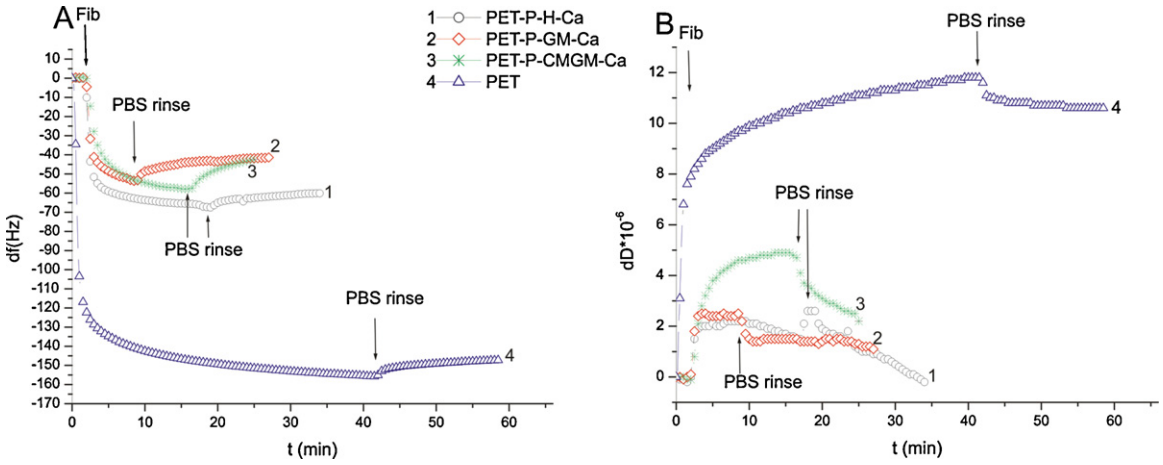

Fig. 8. Frequency (A) and dissipation (B) changes as a function of time during fibrinogen adsorption onto model PET-P surfaces coated with heparin (H), sulphated GM, and sulphated CMGM in the presence of Ca^{2+}.

No significant differences in frequency changes could be noted in comparison to the samples adsorbed to PET in the presence of Ca^{2+} (Fig. 4).

The same trends in $\Delta D = f(\Delta f)$ plots were noticed in the case of PET films modified with sulphated polysaccharides in the presence of Ca^{2+} ions.

The slopes of $\Delta D = f(\Delta f)$ functions of fibrinogen adsorption (Fig. 7) showed the same values as in the previous case (0.05×10^{-6}/Hz in Fig. 5) and therefore indicate a less densely adsorbed layer. Those $\Delta D = f(\Delta f)$ functions displayed simple behaviour with a linear relationship.

When polysaccharides were adsorbed onto PET-P surfaces (Fig. 8) in the presence of calcium chloride, forming thicker adsorption layers, fibrinogen adsorption decreased by about 40% in comparison to the samples treated in the absence of calcium chloride (Fig. 6).

Fibrinogen adsorbed onto the PET-P surfaces modified with polysaccharides in the presence of Ca^{2+} ions showed slightly different slope values in comparison to adsorption onto the PET surfaces and PET-P surfaces where no calcium chloride was used. The slopes differ from one polysaccharide to another. The PET-P-H-Ca sample showed the lowest slope (0.035×10^{-6}/Hz), for the PET-P-GM-Ca sample the slope was 0.06×10^{-6}/Hz, and for the PET-P-CMGM-Ca sample the slope was the highest (0.085×10^{-6}/Hz), which is very close to the k_0 value (0.09×10^{-6}/Hz). In all these three cases, the adsorbed fibrinogen layer was softer, suggesting the layer had a water rich structure. Most of the other samples showed a slope of 0.05×10^{-6}/Hz similar to PET-P-GM-Ca, only PET-P-CMGM-Ca was softer, and PET-P-H-Ca was the most rigid.

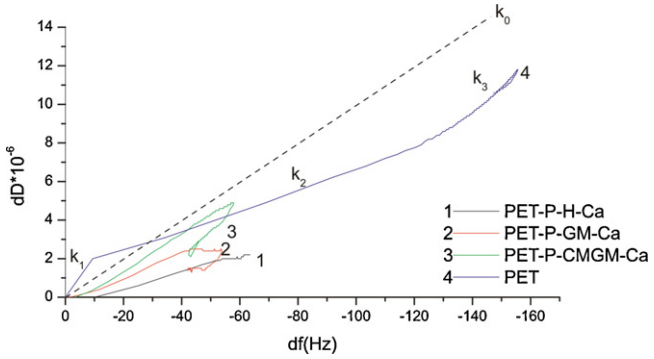

Fig. 9. $\Delta D = f(\Delta f)$ functions of fibrinogen adsorption onto model PET-P films modified with polysaccharides in the presence of Ca^{2+} (k_1, k_2 and k_3 – different slopes of the plot 4; k_0 – theoretical function slope, which indicates the boundary between soft and rigid adsorbed layers).

3.5. Evaluation of adsorbed fibrinogen layers' thicknesses

The thicknesses of the adsorbed fibrinogen layers were evaluated with the help of QTools software using the Voight viscoelastic model and the Sauerbrey equation. The Sauerbrey equation is usually used when dissipation change is low, $\Delta D_n/(\Delta f_n/n) \ll 0.4 \times 10^{-6}$/Hz (Reviakine, Johannsmann, & Richter, 2011). As suggested by the QCM-D producer (QSense), the Sauerbrey equation can be applied when ΔD is less than 1×10^{-6} per every 10 Hz in frequency change (this is the slope of the k_0 function). The Sauerbrey equation considers only frequency changes for the calculation of an adsorbed layer's thickness; therefore in cases of viscoelastic films, where dissipations are much higher, this approach is not the right method of evaluation.

For evaluation of the systems where the slope of the function $\Delta D = f(\Delta f)$ is higher than 0.099, the Voight viscoelastic model was developed to obtain more accurate results.

Owing to this fact, in this research modelling with QTools was applied where the frequency and dissipation changes for overtones from no. 3 up to no. 9 were considered as well.

The unknown parameters can be extracted by fitting experimental frequency and dissipation data from 2 or more harmonics (Fig. 10).

The spin coated model PET films with adsorbed anticoagulant polysaccharides, which are rigid and evenly distributed, were treated as the quartz crystal. Owing to this very complex system, some simplifications were used in the modelling: the adsorbed protein layers were treated as homogeneous layers between the QCM sensor (quartz crystal + PET film) and a semi-infinite Newtonian liquid layer under a non-slip boundary condition. The density (1000 kg/m^3) and viscosity (0.001 kg/ms) of water were used for all of the bulk liquids, and the density of the adsorbed protein (fibrinogen) layer was fixed to 1150 kg/m^3, corresponding to a densely packed low hydrated protein film (Höök et al., 2001).

In Fig. 11 the thicknesses of the polysaccharide and protein layers calculated on the basis of the Sauerbrey equation and the Voight viscoelastic model are presented. Larger differences between the results obtained by different evaluation approaches indicate higher softness of the layers.

Fibrinogen adsorption was significantly influenced by surface modification using anticoagulant polysaccharides (Fig. 11). The

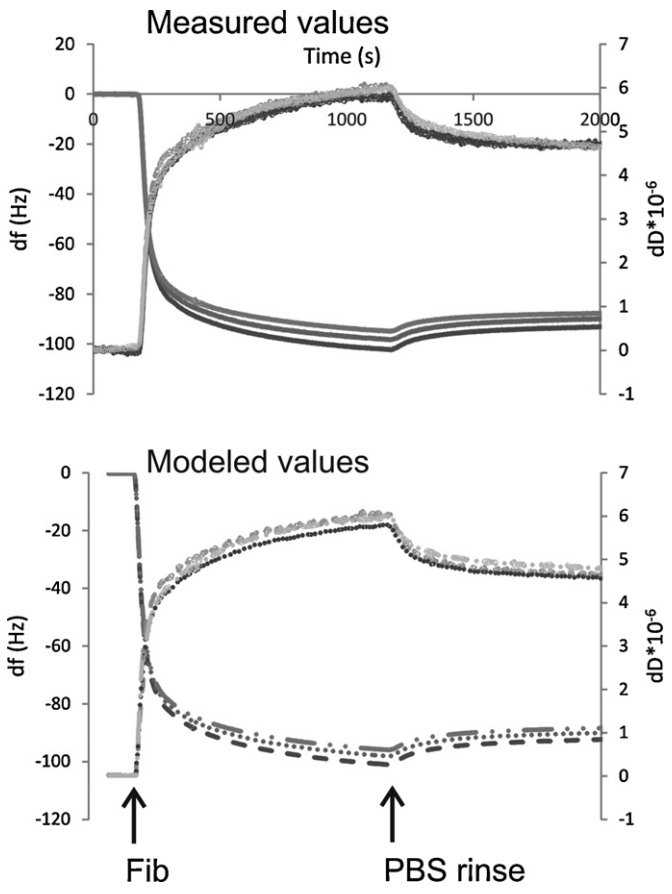

Fig. 10. Example of modelling of the measured Δf and ΔD values for the PET-P-H sample for the 3rd, 5th and 7th overtones.

fibrinogen layers on the polysaccharide surfaces were, by 35–80%, thinner than in the case of non-modified PET film.

In the cases of fibrinogen either adsorbed on PET in the presence of Ca^{2+} or on the PET-P surface, almost identical layer thicknesses were determined, independent of the nature of the PS. The thickness of the adsorbed fibrinogen layers calculated using the Voight approach (19–28 nm) or using the Sauerbrey approach (12–19 nm) differ significantly. The PS substrate always showed layer thicknesses between 2 and 4 nm. This indicates that the adsorbed layers had softer structures (less elastic, more viscous) with a significant amount of embedded water.

Fibrinogen adsorption on the PET-P substrates was different if Ca^{2+} was present (PET-P-H-Ca, PET-P-GM-Ca and PET-P-CMGM-Ca samples). This resulted in much thicker anticoagulant polysaccharide layers (8–14 nm instead of 3 nm) and a decrease in the adsorbed fibrinogen layer's thickness by about 60–80% (7–14 nm). The differences between the Voight and Sauerbrey results more or less vanish.

When comparing the thicknesses from the Voight based and Sauerbrey calculations, they were not significantly different in the cases when the polysaccharides were adsorbed on PET-P in the presence of Ca^{2+}. In case of PET-P-GM-Ca, the difference between Voight and Sauerbrey calculation did not follow that trend; in this case the difference is higher, suggesting softer protein layer. In case of PET-P-H-Ca and PET-P-CMGM-Ca samples the resulting protein layer was more dense and rigid, with less water incorporated.

Recent studies (Bajpai, 2008; Wertz & Santore, 1999, 2001a, 2001b) have revealed that fibrinogen can exist in many possible orientations and/or conformations depending on the adsorption condition and surface chemical and physical properties of the substrate. The hydrodynamic radius of the fibrinogen molecule in PBS was determined to be 12.7 nm (Wasilewska, Adamczyk, & Jachimska, 2009), and the estimated thicknesses of the fibrinogen layers for PS coated surfaces on the PET-P surface in the presence of Ca^{2+} were similar.

It has been shown (Bai, Filiaggi, & Dahn, 2009; Siegismund, Keller, Jandt, & Rettenmayr, 2010) that fibrinogen at the concentration used (1 mg/mL) adsorbs on most surfaces following the Langmuir adsorption isotherm, where only monolayer is formed at maximal adsorption. The results of this research showed that the adsorbed fibrinogen layer is thicker when adsorbed onto non-modified PET film. We assumed that the fibrinogen molecules in this case formed monolayers with an end-on molecular orientation from the PET surface into the solution; thus the layers' thicknesses were in the range of the fibrinogen molecules' lengths (Fig. 12B). The outermost layer may be an additional soft fibrinogen layer containing significant amounts of water. This is indicated by the slope of the dissipation via the frequency function. This was the case after rinsing with PBS app. 0.13×10^{-6} (function 4 in Figs. 5, 7 and 9).

In the case of the thin (3 nm) PS layers adsorbed on the PET surface in the presence of Ca^{2+} and on the PET-P surface (without Ca^{2+}) one single layer of loosely packed fibrinogen molecules in an end-on structure is most likely formed on the surface (fibrinogen

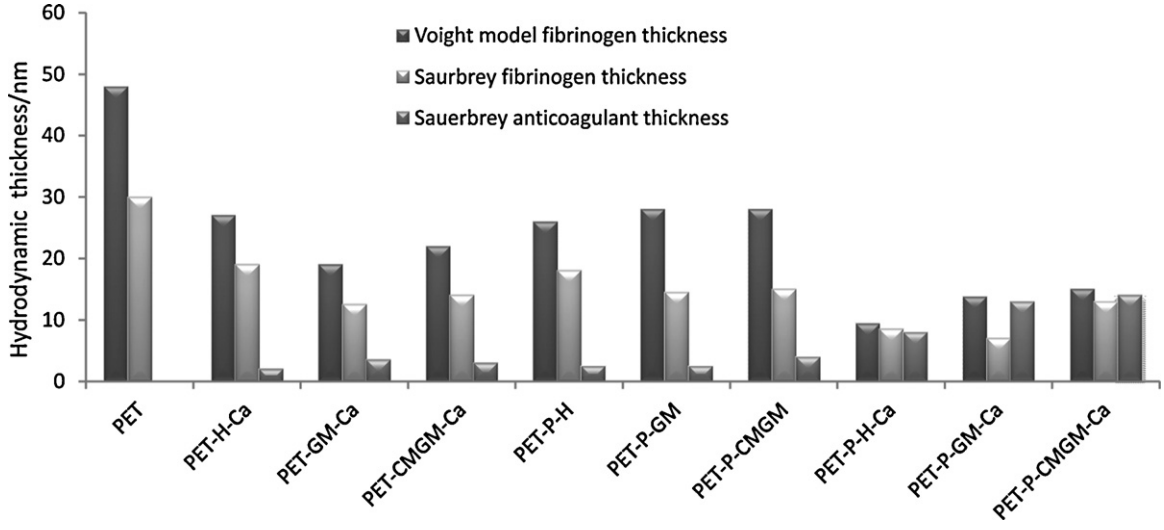

Fig. 11. The thicknesses of adsorbed anticoagulant polysaccharide and fibrinogen layers evaluated by the Sauerbrey equation or the Voight viscoelastic model.

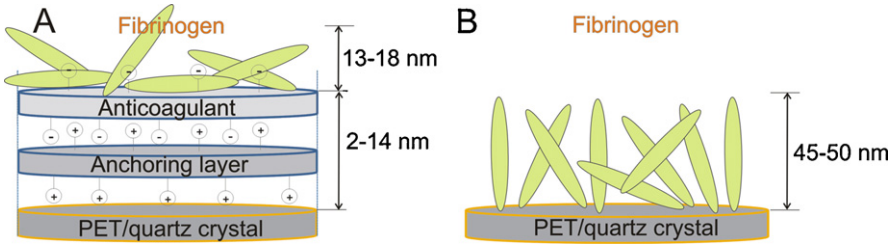

Fig. 12. A hypothetical model of fibrinogen adsorption onto PET films.

length was 45 nm). This is indicated in all three cases (PET, PET-PS-Ca, PET-P-PS) by the slopes of the $\Delta D = f(\Delta f)$ functions as well as by the big differences between the thicknesses obtained via the Voight and the Sauerbrey approaches. The fibrinogen molecules may in one case interact directly with the negatively charged PS layer, in the other case they may interact with the PS layer due to charge screening/intermediation via the bi-valent Ca^{2+} ions.

The adsorbed fibrinogen layers on the PET-P samples modified with polysaccharides in the presence of Ca^{2+} were much thinner. The thicknesses of these layers on PET-P in the presence of Ca^{2+} were around 13 nm, and the layers were more rigid (Fig. 11). For these layers a side-on orientation for most of the adsorbed fibrinogen molecules on the thick (13 nm) PS layer can be suggested (Fig. 12A). The reason might be the PS film's rather soft outer layer, which offers many places for electrostatic interactions, binding in this way a thin, rather rigid fibrinogen layer in a side-on orientation.

4. Summary and conclusions

In this research the adsorption of blood protein fibrinogen onto model PET and cationic PET-P surfaces coated with different anticoagulant PS was investigated using quartz crystal microbalance with dissipation unit.

The coating process was monitored using contact angle and AFM. The PET film's static water contact angle decreased only slightly in the case of adsorbed heparin; the adsorption of sulphated galactoglucomannan and sulphated carboxylmethyl galactoglucomannan led to a decrease of about 23%. The highest hydrophilicities were achieved with polysaccharide layers when calcium chloride was present in the polysaccharide solutions during adsorption. AFM images and the calculated average roughness (Sa) after the polysaccharides' adsorption onto the model PET surfaces showed significant differences between the non-modified and modified surfaces.

The results of the protein adsorption experiments showed that fibrinogen adsorption, which is usually correlated with the haemocompatibility of PET surfaces, can be tuned by coating layers of sulphated polysaccharides with anticoagulant properties. The thickest anticoagulant layers were achieved using the cationic polymer PEI as PS anchor groups in the presence of Ca^{2+}. This combination led to the thinnest layers of adsorbed fibrinogen.

Evaluation of the QCM-D data using the viscoelastic model (Voight) showed that the nature of fibrinogen adsorption and the properties of the adsorbed layer depend strongly on the PET coating.

In the case of PET surfaces coated with anticoagulant polysaccharides in the presence of Ca^{2+} or PET-P surfaces coated with anticoagulant polysaccharides, the fibrinogen layers were 35–80% thinner than in the case of the non-modified PET film. When comparing the thicknesses using the Voight and Sauerbrey approaches, they were significantly different. This indicates that the resulting protein layer is not rigid; it acts as a viscoelastic system dissipating energy via viscous deformation.

The formation of a fibrinogen layer on a PET-P anticoagulant PS layer in the presence of Ca^{2+} led to a denser and more rigid protein structure with less water incorporated. This layer acts more as an elastic system, less able to disseminate energy via viscous deformation.

It can be concluded that protein layers with different viscoelastic properties are formed on PET surfaces depending on the nature of the primary substrate layers (anticoagulant PS) coated on the PET surface. The results suggest different orientations as well as densities resulting in different viscoelasticities of the adsorbed fibrinogen layers.

The adsorption of fibrinogen can be used as a quick indication of surface haemocompatibility determination, and using a Voight based viscoelastic model realistic protein thickness on a surface can be estimated.

Acknowledgement

The research leading to these results has received funding from the European Union Seventh Framework Programme (FP7/2007-2013) under grant agreement nr. 214653.

References

Bai, Z., Filiaggi, M. J., & Dahn, J. R. (2009). Fibrinogen adsorption onto 316L stainless steel, Nitinol and titanium. *Surface Science*, *603*(6), 839–846.

Bajpai, A. K. (2008). Fibrinogen adsorption onto macroporous polymeric surfaces: Correlation with biocompatibility aspects. *Journal of Materials Science-Materials in Medicine*, *19*(1), 343–357.

Cacciafesta, P., Humphris, A. D. L., Jandt, K. D., & Miles, M. J. (2000). Human plasma fibrinogen adsorption on ultraflat titanium oxide surfaces studied with atomic force microscopy. *Langmuir*, *16*(21), 8167–8175.

Dário, A. F., Hortêncio, L. M. A., Sierakowski, M. R., Neto, J. C. Q., & Petri, D. F. S. (2011). The effect of calcium salts on the viscosity and adsorption behavior of xanthan. *Carbohydrate Polymers*, *84*(1), 669–676.

Doliška, A., Willför, S., Strnad, S., Ribitsch, V., Kleinschek, K. S., Eklund, P., et al. (2011). Antithrombotic properties of sulfated wood-derived galactoglucomannans. *Holzforschung*, *66*(2), 149–154.

Fasl, H., Stana, J., Stropnik, D., Strnad, S., Stana-Kleinschek, K., & Ribitsch, V. (2010). Improvement of the hemocompatibility of PET surfaces using different sulphated polysaccharides as coating materials. *Biomacromolecules*, *11*(2), 377–381.

Gericke, M., Doliska, A., Stana, J., Liebert, T., Heinze, T., & Stana-Kleinschek, K. (2011). Semi-synthetic polysaccharide sulfates as anticoagulant coatings for PET, 1 – Cellulose sulfate. *Macromolecular Bioscience*, *11*(4), 549–556.

Guicai, L., Xiaoli, S., Ping, Y., Ansha, Z., & Nan, H. (2008). Investigation of fibrinogen adsorption on solid surface by quartz crystal microbalance with dissipation (QCM-D) and ELISA. *Solid State Ionics*, *179*(21–26), 932–935.

Hemmersam, A. G., Foss, M., Chevallier, J., & Besenbacher, F. (2005). Adsorption of fibrinogen on tantalum oxide, titanium oxide and gold studied by the QCM-D technique. *Colloids and Surfaces B-Biointerfaces*, *43*(3–4), 208–215.

Holmberg, K., Jönsson, B., Kronberg, B., & Lindmann, B. (2003). *Surfactants and polymers in aqueous solution* (pp. 403–435).(2nd ed.). West Sussex, England: John Wiley & Sons Ltd.

Höök, F., Kasemo, B., Nylander, T., Fant, C., Sott, K., & Elwing, H. (2001). Variations in coupled water, viscoelastic properties, and film thickness of a Mefp-1 protein film during adsorption and cross-linking: A quartz crystal microbalance with dissipation monitoring, ellipsometry, and surface plasmon resonance study. *Analytical Chemistry*, *73*(24), 5796–5804.

Imai, Y., & Nose, Y. (1972). A new method for evalution of antithrombogenicity of materials. *Journal of Biomedical Materials Research*, *6*(3), 165–172.

Indest, T. (2007). *Study of polyethylene terephthalate surface treatment with polysaccharides for medical application* (p. 156). Maribor: University of Maribor.

Indest, T., Laine, J., Johansson, L. S., Stana-Kleinschek, K., Strnad, S., Dworczak, R., et al. (2009). Adsorption of fucoidan and chitosan sulfate on chitosan modified PET films monitored by QCM-D. *Biomacromolecules*, *10*(3), 630–637.

Indest, T., Laine, J., Kleinschek, K. S., & Zemljic, L. F. (2010). Adsorption of human serum albumin (HSA) on modified PET films monitored by QCM-D, XPS and AFM. *Colloids and Surfaces A-Physicochemical and Engineering Aspects*, *360*(1–3), 210–219.

Irwin, E. F., Ho, J. E., Kane, S. R., & Healy, K. E. (2005). Analysis of interpenetrating polymer networks via quartz crystal microbalance with dissipation monitoring. *Langmuir*, *21*(12), 5529–5536.

Kannan, R. Y., Salacinski, H. J., Vara, D. S., Odlyha, M., & Seifalian, A. M. (2006). Review paper: Principles and applications of surface analytical techniques at the vascular interface. *Journal of Biomaterials Applications*, *21*(1), 5–32.

Keuren, J. F. W., Wielders, S. J. H., Willems, G. M., Morra, M., Cahalan, L., Cahalan, P., et al. (2003). Thrombogenicity of polysaccharide-coated surfaces. *Biomaterials*, *24*(11), 1917–1924.

Kou, J., Tao, D., & Xu, G. (2010). A study of adsorption of dodecylamine on quartz surface using quartz crystal microbalance with dissipation. *Colloids and Surfaces A: Physicochemical and Engineering Aspects*, *368*(1–3), 75–83.

Kristensen, E. M. E., Rensmo, H., Larsson, R., & Siegbahn, H. (2003). Characterization of heparin surfaces using photoelectron spectroscopy and quartz crystal microbalance. *Biomaterials*, *24*(23), 4153–4159.

Laos, K., Parker, R., Moffat, J., Wellner, N., & Ring, S. G. (2006). The adsorption of globular proteins, bovine serum albumin and [beta]-lactoglobulin, on poly-L-lysine-furcellaran multilayers. *Carbohydrate Polymers*, *65*(3), 235–242.

Liu, Y., He, T., & Gao, C. (2005). Surface modification of poly(ethylene terephthalate) via hydrolysis and layer-by-layer assembly of chitosan and chondroitin sulfate to construct cytocompatible layer for human endothelial cells. *Colloids and Surfaces B: Biointerfaces*, *46*(2), 117–126.

Liu, Z., Choi, H., Gatenholm, P., & Esker, A. R. (2011). Quartz crystal microbalance with dissipation monitoring and surface plasmon resonance studies of carboxymethyl cellulose adsorption onto regenerated cellulose surfaces. *Langmuir*, *27*(14), 8718–8728.

Nishino, T., Aizu, Y., & Nagumo, T. (1991). Antithrombin activity of a fucan sulfate from the brown seaweed Ecklonia kurome. *Thrombosis Research*, *62*(6), 765–773.

Nishino, T., & Nagumo, T. (1992). Anticoagulant and antithrombin activities of oversulfated fucans. *Carbohydrate Research*, *229*(2), 355–362.

Ratner, B. D. (2007). The catastrophe revisited: Blood compatibility in the 21st century. *Biomaterials*, *28*(34), 5144–5147.

Reviakine, I., Johannsmann, D., & Richter, R. P. (2011). Hearing what you cannot see and visualizing what you hear: Interpreting quartz crystal microbalance data from solvated interfaces. *Analytical Chemistry*.

Sanchez, J., Elgue, G., Riesenfeld, J., & Olsson, P. (1995). Control of contact activation on end-point immobilized heparin: The role of antithrombin and the specific antithrombin-binding sequence. *Journal of Biomedical Materials Research*, *29*(5), 655–661.

Sanchez, J., Elgue, G., Riesenfeld, J., & Olsson, P. (1998). Studies of adsorption, activation, and inhibition of factor XII on immobilized heparin. *Thrombosis Research*, *89*(1), 41–50.

Sauerbrey, G. Z. (1959). Phys., 155(2), 206%U http://dx.doi.org/210.1007/BF01337937 %@ 01331434-01336001.

Seyfert, U., Biehl, V., & Schenk, J. (2002). In vitro hemocompatibility testing according to ISO 10993-4. *Biomolecular Engineering*, *19*(91–96)

Siegismund, D., Keller, T. F., Jandt, K. D., & Rettenmayr, M. (2010). Fibrinogen adsorption on biomaterials – A numerical study. *Macromolecular Bioscience*, *10*(10), 1216–1223.

Sit, P. S., & Marchant, R. E. (1999). Surface-dependent conformations of human fibrinogen observed by atomic force microscopy under aqueous conditions. *Thrombosis and Haemostasis*, *82*(3), 1053–1060.

Streller, U., Sperling, C., Hübner, J., Hanke, R., & Werner, C. (2003). Design and evaluation of novel blood incubation systems for in vitro hemocompatibility assessment of planar solid surfaces. *Journal of Biomedical Materials Research Part B: Applied Biomaterials*, *66B*(1), 379–390.

Takemoto, S., Yamamoto, T., Tsuru, K., Hayakawa, S., Osaka, A., & Takashima, S. (2004). Platelet adhesion on titanium oxide gels: Effect of surface oxidation. *Biomaterials*, *25*(17), 3485–3492.

Vogt, B. D., Lin, E. K., Wu, W.-l., & White, C. C. (2004). Effect of film thickness on the validity of the Sauerbrey equation for hydrated polyelectrolyte films. *The Journal of Physical Chemistry B*, *108*(34), 12685–12690.

Voinova, M. V., Rodahl, M., Jonson, M., & Kasemo, B. (1999). Viscoelastic acoustic response of layered polymer films at fluid–solid interfaces: Continuum mechanics approach. *Physica Scripta*, *59*, 391–396.

Wasilewska, M., Adamczyk, Z., & Jachimska, B. (2009). Structure of fibrinogen in electrolyte solutions derived from dynamic light scattering (DLS) and viscosity measurements. *Langmuir*, *25*(6), 3698–3704.

Weber, N., Wendel, H. P., & Kohn, J. (2005). Formation of viscoelastic protein layers on polymeric surfaces relevant to platelet adhesion. *Journal of Biomedical Materials Research A*, *72A*(4), 427.

Wertz, C. F., & Santore, M. M. (1999). Adsorption and relaxation kinetics of albumin and fibrinogen on hydrophobic surfaces: Single-species and competitive behavior. *Langmuir*, *15*(26), 8884–8894.

Wertz, C. F., & Santore, M. M. (2001a). Effect of surface hydrophobicity on adsorption and relaxation kinetics of albumin and fibrinogen: Single-species and competitive behavior. *Langmuir*, *17*(10), 3006–3016.

Wertz, C. F., & Santore, M. M. (2001b). Fibrinogen adsorption on hydrophilic and hydrophobic surfaces: Geometrical and energetic aspects of interfacial relaxations. *Langmuir*, *18*(3), 706–715.

Willför, S., Rehn, P., Sundberg, A., Sundberg, K., & Holmbom, B. (2003). Recovery of water-soluble acetylgalactoglucomannans from mechanical pulp of spruce. *TAPPI Journal*, *2*(11).

Wu, Y., Simonovsky, F. I., Ratner, B. D., & Horbett, T. A. (2005). The role of adsorbed fibrinogen in platelet adhesion to polyurethane surfaces: A comparison of surface hydrophobicity, protein adsorption, monoclonal antibody binding, and platelet adhesion. *Journal of Biomedical Materials Research A*, *74*(4), 722–738.

Yu, L. J., Wang, X., Wang, X. H., & Liu, X. H. (2000). Haemocompatibility of tetrahedral amorphous carbon films. *Surface & Coatings Technology*, *128*, 484–488.

Zhang, Z., Zhang, M., Chen, S., Horbett, T. A., Ratner, B. D., & Jiang, S. (2008). Blood compatibility of surfaces with superlow protein adsorption. *Biomaterials*, *29*(32), 4285–4291.